Lidar-based Mapping of Forest Volume and Biomass by Taxonomic Group Using Structurally Homogenous Segments

Jan A.N. van Aardt, Randolph H. Wynne, and John A. Scrivani

Abstract

This study evaluated the potential of an object-oriented approach to forest type classification as well as volume and biomass estimation using small-footprint, multiple return lidar data. The approach was applied to coniferous, deciduous, and mixed forest stands in the Virginia Piedmont, U.S.A. A multiresolution, hierarchical segmentation algorithm was applied to a canopy height model (CHM) to delineate objects ranging from 0.035 to 5.632 ha/average object. Per-object lidar point (per return height and intensity) and CHM distributional parameters were used as input to a discriminant classification of 2-class (deciduous-coniferous) and 3-class (deciduous-coniferous-mixed) forest definitions. Lidar point-height-based and CHM classifications yielded overall accuracies of 89 percent and 79 percent, respectively. Volume and biomass estimates exhibited differences of no more than 5.5 percent compared to field estimates, while showing distinctly improved precisions (up to 45.5 percent). There were no significant differences between accuracies for varying object sizes, which implies that reducing the lidar point coverage would not affect classification accuracy. These results lead to the conclusion that a lidar-based approach to forest type classification and volume/biomass assessment has the potential to serve as a single-source inventory tool.

Introduction

Accurate forest inventory and forest type discrimination, defined here as the distinction between deciduous and coniferous species, are crucial to forest growth stock management, carbon sequestration monitoring, wildlife habitat definition, and management of human impacts on a forest environment. Generally speaking, however, forest assessment remains challenging for vast tracts of land where accessibility may be limited. Remote sensing offers a solution in that inventory and classification outputs, based on earth observation approaches, enable managers to derive forest volume-by-type maps from imagery. Previous remote sensing-based forest assessments have focused on using multispectral data as inputs to classification (e.g., Franklin, 1994; White *et al.*, 1995) and inventory (e.g., Ardö, 1992; Avery and Burkhart, 1994). Light detection and ranging (lidar) approaches, however, recently have come to the fore where forest type discrimination (Douglas *et al.*, 2003) and volume estimation (e.g., Lefsky *et al.*, 1999; Popescu *et al.*, 2004) are concerned. Remote sensing approaches primarily have been pixel- or stand-based, while object-based classification has gained popularity as an alternative method (Heyman *et al.*, 2003).

Object-based classification approximates real-world object classification, with procedures applied to homogenous units. An object here refers to a spatial entity that is homogenous in terms of a selected property, as opposed to continuous fields (Burrough and McDonnell, 1998). Results also are representative of real-world objects and very often are devoid of the salt-and-pepper appearance that is typical of pixel-based classifiers. While accuracies of pixel-based and object-oriented approaches are similar in many cases, the realistic classification rendering of the object-oriented approach is of importance (White *et al.*, 1995; Heyman *et al.*, 2003). Benz *et al.* (2004) highlight the importance of linkages between real-world objects, knowledge-based image interpretation, and the selection and combination of scales, all of which are applicable to natural resource managers. The authors underline the importance of these attributes in instances where scalability is essential, e.g., between sub-stand and stand-level in the forestry context, and where objects encompass operational units that are defined by a natural resource manager.

Derivation of unique objects or segments is required as a precursor to any per-object analysis. Established segmentation approaches include the Woodcock-Harward centroid-linkage algorithm (Shandley *et al.*, 1996), Markov random field model-based segmentation (Smits and Dellepiane, 1997), a Hough transformed-based approach (Shankar *et al.*, 1998), watershed-based hierarchical segmentation (Li *et al.*, 1999), and multiresolution, hierarchical segmentation (Baatz and Schäpe, 2000), among others. Many studies have applied segmentation as a preprocessing step to forest classification (Jaakkola,

Jan A.N. van Aardt is with the Council for Scientific and Industrial Research, Ecosystem Earth Observation, P.O. Box 395, Pretoria, 0001, South Africa, and formerly with the Department of Forestry, Virginia Polytechnic Institute and State University (jvaardt@csir.co.za).

Randolph H. Wynne is with the Department of Forestry, Virginia Polytechnic Institute and State University, 319 Cheatham Hall (0324), Blacksburg, VA 24060.

John A. Scrivani is with the Virginia Department of Forestry, 900 Natural Resources Drive, Suite 800, Charlottesville, VA 22903.

Photogrammetric Engineering & Remote Sensing
Vol. 74, No. 8, August 2008, pp. 1033–1044.

0099-1112/08/7408–1033/$3.00/0

1989; Kayitakire *et al.*, 2002; Dorren *et al.*, 2003; Budreski *et al.*, 2007), as well as other object-based analyses, e.g., forest loss detection (Abkar *et al.*, 2000) and per-object volume estimation (Pekkarinen, 2002). Object-oriented approaches to forest classification generally performed well when compared to more traditional, pixel-based approaches (e.g., Heyman *et al.*, 2003).

Although previous studies have found acceptable per-object classification accuracies, multiple data sources, such as optical and lidar data, are often required if the goal extends past classification (Dorren *et al.*, 2003) to biophysical parameter modeling (Næsset, 2002). Douglas *et al.* (2003), however, used lidar canopy density and intensity, derived from small footprint lidar data, to classify mature pine, immature pine, and mature hardwood stands in Mississippi. Analyses were limited to the forest canopy by only using lidar returns in the upper 50 percent of the total tree height. The authors used a discriminant classification with the number of lidar hits per cubic meter and the variance of the intensity data within the canopy of each plot as variables. Accuracies of 100 percent (mature pine), 85.7 percent (immature pine), and 93.3 percent (mature hardwood) were achieved, with an overall accuracy of 86.4 percent. Although not object-based, Brandtberg (2007) increased leaf-off individual tree species classification from 60 percent to 64 percent using a directed graph approach applied to small-footprint two-return lidar data in West Virginia, U.S.A. The species in question were *Quercus* spp. (oaks), *Acer rubrum* (red maple), and *Liriodendron tulipifera* (yellow poplar). These results bode well for the application of lidar data, a structural data source due to its height information, to forest classification. Logical extensions of a lidar-based classification include (a) the use of complete lidar distributional data, not limited to canopy returns, (b) implementation of a range of distributional parameters, e.g., range, mode, skewness, kurtosis, and percentiles, and (c) the evaluation of lidar-based, object-oriented forest classification, an attractive goal given the scalability of results through recombination of objects. Extension of this data source to classification has far reaching consequences, based on the additional applicability of lidar data to the measurement of forest biophysical parameters. Lidar data conceivably could form the basis of a complete per-object, forest inventory. However, this approach requires associated per-object volume and/or biomass estimation.

Although many researchers have shown the utility of lidar to model forest heights and volume (e.g., Nelson *et al.*, 1988; Lefsky *et al.*, 1999; Popescu *et al.*, 2004), small-footprint, discrete return studies that rely on distributional approaches are rare. Means *et al.* (2000) and Næsset (2002) implemented lidar distributional approaches to estimate basal area ($R^2 = 0.97$) of Douglas-fir stands, and volume ($R^2 = 0.91$) of Norway spruce (*Picea abies*) and Scots pine (*Pinus sylvestris*) stands, respectively. Associated standard deviations between 18.3 and 31.9 m^3/ha proved the usefulness of this type of approach. These lidar distributional approaches subsequently were extended to object-level volume/biomass modeling in the Virginia Piedmont, U.S.A., by van Aardt *et al.* (2006). The authors showed that although adjusted R^2 values (0.58 to 0.79; various object sizes) were relatively low due to the variable forest structure within a relatively narrow biomass range, RMSE values (28.02 to 55.98 m^3/ha and 12.06 to 39.48 Mg/ha) were amenable to operational volume and biomass modeling.

The main objective of this study was to assess the potential utility of lidar-based, per-object classification for mapping 2-class (deciduous-coniferous) and 3-class (deciduous-coniferous-mixed) objects in the Virginia Piedmont. A secondary objective involved the comparison of discriminant classification using lidar point (per return height and intensity) distributions on the one hand, and height distributions derived from a 1 m canopy height model (CHM) on the other. The final objective was to evaluate the combination of such classifications with object-based volume and biomass modeling using lidar distributions, based on models published by van Aardt *et al.* (2006). Addressing these three goals could help in determining the extent to which lidar data can be used as single remote sensing data source for forest type discrimination and biophysical parameter modeling (Næsset, 2002; Popescu *et al.*, 2002).

Methods

The 946 ha (2,338 acres) study area is located in Appomattox Buckingham State Forest (Appomattox and Buckingham Counties) in the Piedmont physiographic province of Virginia, southeastern U.S.A. at 78°41′ W, 37°25′ N (Figure 1). The mean elevation of the study area is 185 m (606 ft.), with minimum and maximum elevations of 133 m (436 ft.) and 225 m (738 ft.), respectively. Local topography can best be described as gentle rolling slopes and flat terrain. Vegetation is composed of various coniferous (*Pinus taeda, P. virginiana, P. echinata*, and *P. strobus*), and deciduous (*Quercus coccinea, Q. alba, Q. velutina, Q. falcata, Q. rubra, Liriodendron tulipifera*, and *Carya* spp.) species.

Lidar data (Table 1) were acquired by Spectrum Mapping, LLC using the DATIS II sensor (small-footprint, high-density, multiple return) on 09 September 2002 centered at 78°40′30″ W, 37°25′9″ N. Field data consisted of 256 basal area plots (BAF; basal area factor 10) on a grid with 16 columns by 16 rows and a between-plot spacing of 201.17 m (10 chains). Field data were collected during the summer, fall, and winter months (May to December) of 2003. GPS (differentially-corrected) location, basal area, diameter at breast height (DBH), height, and species were determined for all plots and tallied trees. A total of 219 BAF plots ultimately were used in the statistical analysis, since 37 plots were located on private land or had basal area values of zero, which made type assignment impossible for those plots.

Since field plot data intended for model development and validation were used on a per-object basis, the BAF plots were expanded to a per-hectare basis for each object. This was done using standard BAF expansion equations (van Aardt *et al.*, 2006). Basal area plot estimates also were tallied to derive total volume and biomass for the entire study area (Avery and Burkhart, 1994). Volume and biomass equations (Saucier and Clark, 1985; Clark *et al.*, 1986; Schroeder *et al.*, 1997; Sharma and Oderwald, 2001) for per-tree calculations found in Popescu *et al.* (2004), situated in the same geographical area and based on the same species, were used in this study.

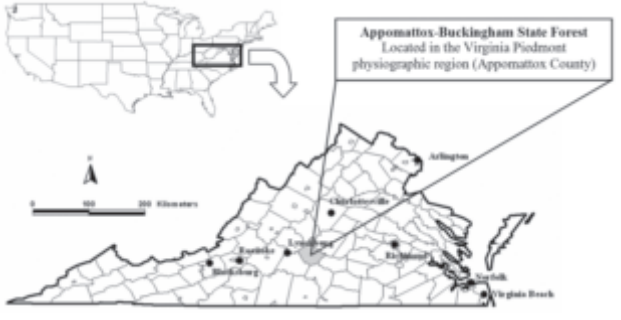

Figure 1. Study Area: Appomattox Buckingham State Forest, Virginia, U.S.A.

TABLE 1. DATIS II LIDAR DATA SET CHARACTERISTICS

Characteristics	Specification
Laser altitude	2,000 m above ground level
Laser scan field-of-view	75° maximum
Swath width and centerline spacing	800 m (2,625 ft.) and 400 m (1,312 ft.)
Scan rate	25 Hz
Laser pulse rate	35 kHz
Scan angle	±13.5°
Returns	≤5
Vertical resolvable distance between returns	0.75 m
Footprint	0.46 m (1.51 ft.)
Average spacing across/along track	1 m (3.3 ft.)/2 m (6.6 ft.)
Accuracy (*X,Y,Z*)	*X,Y*: 0.5 m; *Z*: 0.15 m
Wavelength	1,064 nm

Plots were assigned to 2- and 3-class forest type schemes based on basal area percentages. "Deciduous" or "Coniferous" types were defined as plots that had 50 percent or greater basal area contribution from deciduous or coniferous species, respectively. A "Mixed" class was added to the 3-class type designation for plots that had less than 90 percent basal area contribution for either deciduous or coniferous species. The 2-class analysis consisted of 140 deciduous and 79 coniferous plots, while the 3-class analysis consisted of 112 deciduous, 56 coniferous, and 51 mixed plots. A 90 percent basal area limit was based on plot numbers; there were only 25 mixed plots when a 75 percent cut-off was used, making this class too small for viable statistical analysis. Descriptive statistics for all basal area plots are given in Table 2.

Lidar Data Preprocessing

A canopy height model (CHM) was needed for object derivation as a precursor to per-object classification. First returns were median-filtered by 1 m grid cells in order to remove per-cell values that were redundant to subsequent interpolation procedures. Bare ground returns, based on a proprietary algorithm that incorporates the return number and associated intensity to identify non-vegetation last returns, were provided by the data supplier. First order canopy returns and ground returns, i.e., vegetation-removed last returns, were interpolated (Surfer 7.0 software; Golden Software, Inc.) to 1 m spatial resolution grids using regular Kriging. Popescu *et al.* (2002) found Kriging to be the most accurate interpolation technique using similar data for the same study area. The resultant 1 m resolution of the CHM was detailed enough to detect road and stand breaks in the segmentation process.

The distributional classification approach, based on height distributional parameters, required that lidar data be processed on a per-return basis in order to retain information related to the return hierarchy. Ground hits were removed using Terrascan V. 003.002 (Terrasolid, Inc.) and MicroStation® V. 08.00.04.01 (Bentley Systems, Inc.) software. Ground returns constitute an important component of overall lidar distributional patterns and were retained as data sets on a per-return basis. Non-ground hits, designated as vegetation hits, were normalized (Surfer V. 7.0 software; Golden Software, Inc.) for terrain by calculating the actual return height above a lidar-derived 1 m digital elevation model (DEM) of the study area. This process normalized all vegetation hits for varying terrain elevations, thereby enabling discriminant classification to incorporate actual lidar point-heights in the distributional approach (Means *et al.*, 2000).

Segmentation of the Study Area

Segmentation was performed by applying the eCognition® (eCognition® V. 3.0; Definiens Imaging) multiresolution, hierarchical algorithm to the lidar-derived CHM of the study area. Lidar arguably lends itself to definition of homogenous structural objects through segmentation, given the inherent structural nature of such data. The multiresolution segmentation approach (eCognition® algorithm) considers an entire image, evaluates object homogeneity (within-object variance), shape, compactness, and smoothness, and expands objects across the image to ensure resultant objects of similar size and shape (Baatz and Schäpe, 2000). This algorithm requires Color:Shape and Smoothness:Compactness ratios as input parameters. The

TABLE 2. DESCRIPTIVE STATISTICS ON VOLUME, BIOMASS, AND BASAL AREA FOR 2- AND 3-CLASS PLOT BREAKDOWN

Class	Type	Parameter	Minimum	Maximum	Average	σ
2-class	Deciduous plots (140)	Volume/ha (m^3/ha)	6.9	350.7	157.6	84.1
		Biomass/ha (kg/ha)	11,105.7	269,006.2	113,599.0	58,602.6
		Basal area/ha (m^2/ha)	2.3	34.4	16.3	7.8
	Coniferous plots (79)	Volume/ha (m^3/ha)	8.3	350.9	114.5	75.4
		Biomass/ha (kg/ha)	4668.1	155,558.3	41,468.4	26,641.4
		Basal area/ha (m^2/ha)	2.3	36.7	14.2	7.9
3-class	Deciduous plots (112)	Volume/ha (m^3/ha)	6.9	350.7	156.2	89.3
		Biomass/ha (kg/ha)	11,105.7	269,006.2	117,312.6	62,534.7
		Basal area/ha (m^2/ha)	2.3	34.4	15.0	8.2
	Coniferous plots (56)	Volume/ha (m^3/ha)	8.3	279.1	100.5	66.4
		Biomass/ha (kg/ha)	4,668.1	81,645.1	33,655.4	19,952.0
		Basal area/ha (m^2/ha)	2.3	36.7	13.6	8.1
	Mixed plots (51)	Volume/ha (m^3/ha)	31.7	350.9	156.9	72.6
		Biomass/ha (kg/ha)	20,062.5	175,747.2	81,493.1	38,927.6
		Basal area/ha (m^2/ha)	4.6	36.7	16.8	6.7

Color:Shape ratio was set at 0.8:0.2, based on the recommendation of the developers (Baatz and Schäpe, 2000; eCognition®, 2003) and evaluation of alternative parameter inputs. Object smoothness was considered more important than compactness in a forestry context, since smooth, boundary-following objects are preferable to compact, blocky objects. The Smoothness:Compactness weight combination therefore also was set at 0.8:0.2. It furthermore is important to note that the segmentation method is subordinate in importance to the utility that resultant objects have to analyses. Even though a multitude of segmentation approaches exist in literature (Shandley *et al.*, 1996; Shankar *et al.*, 1998; Li *et al.*, 1999), it is ultimately of great importance that segmentation results are robust. eCognition® was the preferred approach to segmentation because of its hierarchical nature, correspondence to input data, and proven results in the natural resources context (Kayitakire *et al.*, 2002; Nugroho *et al.*, 2002; Kressler *et al.*, 2003). This approach also was selected given that hierarchy theory implies that many natural systems are almost entirely decomposable in subordinate natural objects. This is attributed to the unrestricting vertical and horizontal linkages in structure and function of such systems (Wu, 1999). These attributes are amenable to the forestry and other natural resource contexts, where managers often prefer operations to focus on the largest homogenous unit, which may in turn form part of a larger hierarchy.

The decision of which segmentation results to use for model development was based on between- and within-object variability of the CHM. Classification was performed on segmentation results where within-object variability was smaller than between-object variability, thereby maximizing between-object differences. The smallest selected object sizes corresponded to the areas represented by average tallied tree distance from field-collected BAF plot centers, plus one and two standard deviations. This ensured that objects were representative of plot-level field data, based on corresponding areas. Ten average object sizes, ranging from 0.035 ha/average object to 3.942 ha/average object, were chosen for subsequent forest type classification in order to evaluate classification accuracies across a range of average object sizes. The current Appomattox stand map (167 objects; 5.666 ha/stand) also was selected, as well as the segmentation result that corresponded to the number of operational stands (168 objects; 5.632 ha/average object). Operational stands were used in order to compare segmentation-based classification to stand-based classification. The CHM (1.885 ha/average object result overlaid) and intensity image of the study area are shown in Figure 2.

Vegetation and ground lidar data sets were extracted on a per-object basis for all segmentation results using ArcGIS® V. 8.3 software (ESRI) and exported to SAS V. 8.02 software (Level 02M0; SAS, Inc.) for subsequent discriminant classification. BAF plots were assigned to the object in which they were located through post-stratification. Objects without BAF plots were excluded from the classification process.

Derivation of Per-object Lidar Point and CHM Distributions

Lidar point (per return height and intensity) and CHM (single height layer) distributions were extracted for objects with a forest type assignment (volume greater than zero). Forest type classification was based on the assumption that distinct forest cover and structural types have different, unique distributions or lidar point height densities (Douglas *et al.*, 2003). These distributions can be characterized through construction of per-object height distributions for vegetation returns using the small-footprint DATIS II lidar data (Table 1). Lidar distributions should be representative of unique stand structural characteristics such as canopy closure and stand height distribution. Intermediate return distributions also could be useful, since these returns represent mid-canopy forest structure.

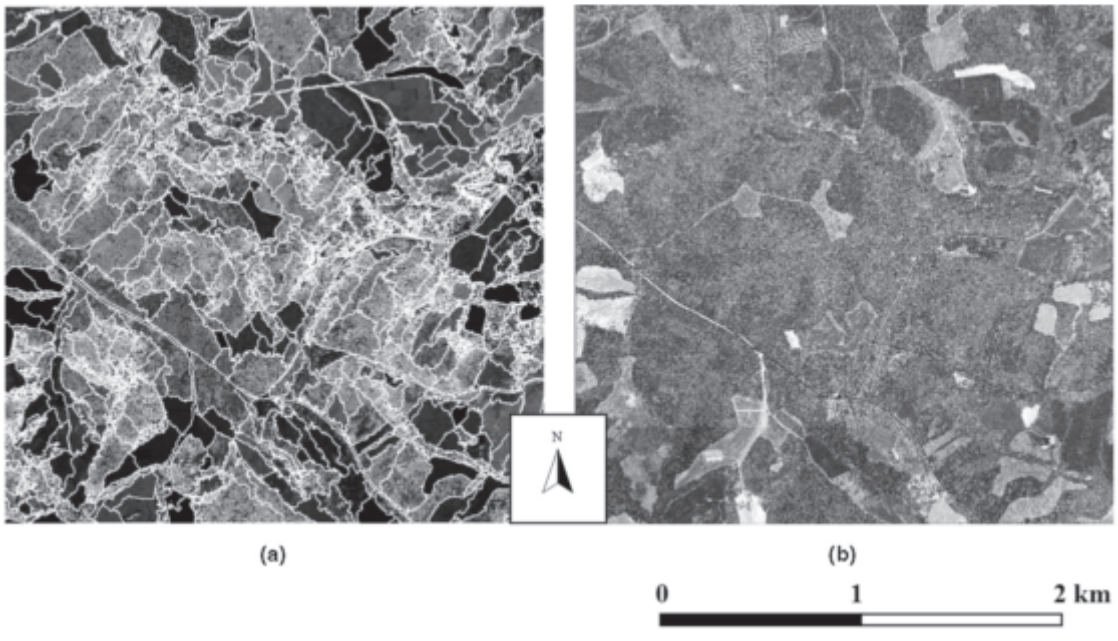

Figure 2. One meter (a) canopy height model, and (b) intensity images of the study area. Higher values are shown in brighter colors in both cases. The 1.885 ha/average object segmentation result is overlaid on (a); this object size resulted in the best classification accuracy.

Only first and second return variables from vegetation return data sets were used because there were many objects with missing values for the third through fifth return data sets. Distributional parameters included the mean, coefficient of variation, kurtosis, maximum, minimum, mode, range, standard error of the mean, skewness, standard deviation, number of observations, height percentile points at 10 percent intervals of height values, and canopy cover percentiles. Canopy cover percentiles, indicative of lidar pulse canopy penetration, were based on the proportion of first returns smaller than a given percentage of maximum height. The ratio of the number of vegetation or ground hits and the total number of lidar hits per object on a per-return basis also were calculated. The vegetation ratio for each object was calculated as the ratio of the total number of vegetation hits per object and the total hits for that object. Figure 3 shows typical first-return distributions for a variety of per-object volume values. Lidar intensity (Figure 2) distributional variables were derived in a similar fashion, but were constrained to per-object CHM heights. Distributional parameters were limited to first return types and canopy cover percentiles, due to the singular nature of the CHM, as opposed to multiple returns found in the case of lidar height points. These types of distribution metrics have been shown to be useful descriptors of stand characteristics for 10 × 10 m grid cells in Douglas-fir (*Pseudotsuga menziesii*) stands in western Oregon (Means *et al.*, 2000), 200 m^2 sample plots in Norway spruce, and Scots pine stands in southeast Norway (Næsset, 2002).

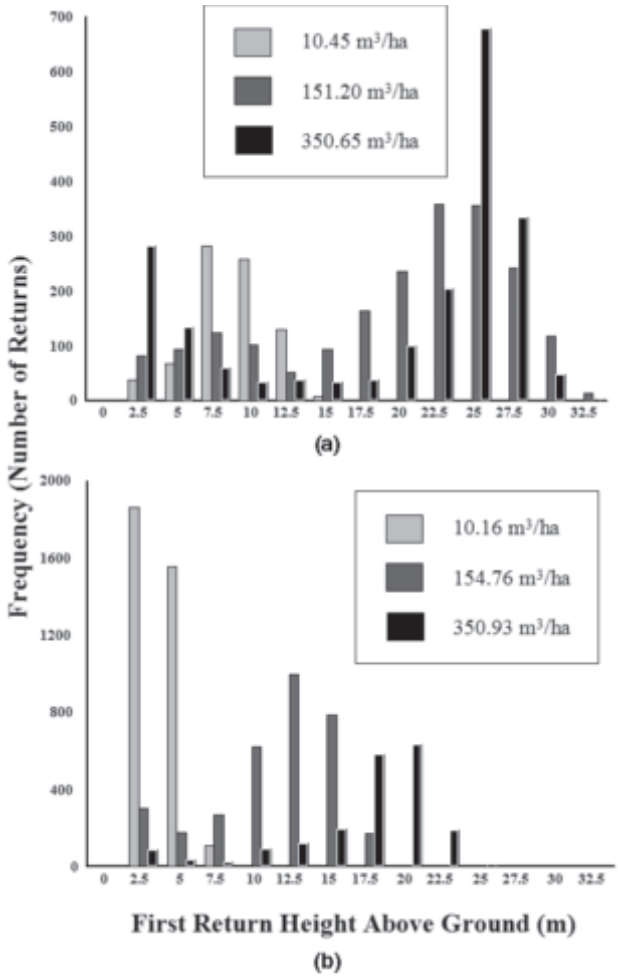

Figure 3. Representative distributions for (a) deciduous, and (b) coniferous per-object (0.035 ha/average object) histogram plots for lidar first return vegetation hits across a range of field-measured volume-per-hectare (van Aardt *et al.*, 2006).

Classification Approach

A discriminant classification approach, similar to the one used by van Aardt and Wynne (2001), was applied to the derived distributional parameters for 2-class (deciduous-coniferous) and 3-class (deciduous- coniferous-mixed) classification schemes. Discriminant approaches, as opposed to non-parametric classifiers, have been shown to be better suited to the classification of high-resolution images where training data have a high degree of overlap in the feature space (Cortijo and De la Blanca, 1999).

General classification statistics, based on cross-validation, included overall accuracy, user's and producer's accuracies, and Kappa-statistics (Congalton and Green, 1999). Comparison between different average object sizes within each classification approach was based on a normalized *z*-test statistic derived from the proportion of correctly classified samples ($\alpha = 0.05$; H_0 = no difference between classification accuracies for different object sizes; H_0 rejected if $z > 1.96$) (Foody, 2004). Samples were treated as independent, since the number of samples for each class was not constant across average object sizes. The standardized normal test statistic for cases with independent test samples are given by:

$$z = \frac{\frac{x_1}{n_1} - \frac{x_2}{n_2}}{\sqrt{p(1-p)\left(\frac{1}{n_1} + \frac{1}{n_2}\right)}} \quad (1)$$

where x_1, x_2 is the correctly allocated number in two independent samples of size n_1 and n_2, respectively, and $p = (x_1 + x_2)/(n_1 + n_2)$ (Foody, 2004).

Significance tests were performed to determine if there were significant differences in (a) accuracies by object size for a given approach, and (b) average accuracies across approaches. Extensive testing was performed since accuracy differences could be significant by chance alone, given the number of possible comparisons among twelve segmentation treatments. Tests were based on a standard t-test ($\alpha = 0.05$) for differences between classification accuracy means (Ott, 1993).

The set of 75 possible point-height classification variables and 31 CHM variables (van Aardt *et al.*, 2006) were reduced to 10 or fewer variables through stepwise discriminant techniques (SAS V. 8.02 software, Level 02M0; SAS, Inc.) using α-levels between 0.1 and 0.35. A simple correlation analysis was performed to evaluate correlations among discriminant variables, with high inter-correlations defined as Pearson's coefficients of 0.8 or higher. A value of 0.8 was chosen based on data characteristics, with the knowledge that all lidar-derived variables are height-related, and hence some correlation was to be expected. Variables with the highest significance to type discrimination were retained based on partial R^2 values. Reduced variable sets were entered into discriminant analyses for 2- and 3-class classification, for each of the segmentation results and for each distributional data type.

Volume and Biomass Estimation Approach

Existing lidar distributional models from van Aardt *et al.* (2006; Table 3), derived using the same distributional approach described in this paper, were used to estimate

TABLE 3. EXAMPLES OF VOLUME MODELS WITH THE HIGHEST ADJUSTED R^2 VALUES FOR 2- AND 3-CLASS SCHEMES (D = DECIDUOUS; C = CONIFEROUS; A = ALL OBJECTS/TYPES; M = MIXED) (VAN AARDT *ET AL.*, 2006)

		Model	Object adjusted R^2	Stand adjusted R^2	Object RMSE (m^3/ha or Mg/ha)	Stand RMSE (m^3/ha or Mg/ha)	Object size (ha)
2-class Volume	D	262.37385 + 19.92957 P_Veg2_70 + 208.14833 ZeroNgrnd3_5ratio − 387.67008 Canopy80P	0.59	0.44	51.15	63.56	5.632
	C	458.52340 − 4.18276 ModeVeg1 + 15.43186 P_Veg1_40 −5.59238 RangeVeg2 −0.36692 StdInt2	0.66	0.48	38.03	55.61	5.632
	A	309.84855 + 0.29731 CVVeg1 + 13.66277 MinVeg1 + 11.12989 P_Veg1_50 −0.14246 MedianInt1 − 432.13149 MinVeg2 + 55.39894 Canopy30P	0.59	0.42	53.75	62.36	0.091
3-class Volume	D	−31.77814 + 19.67658 P_Veg2_70	0.62	0.46	55.98	68.16	5.632
	C	303.72815 + 15.71060 P_Veg1_30 − 1.78646 StdMeanInt2 −0.59669 StdInt2 + 0.06230 MedianInt2 + 737.63803 ZeroNgrnd1ratio + 146.83730 Canopy70P	0.67	0.73	38.24	40.08	0.642
	M	255.71328 −3.17225 ModeVeg1 + 1.54155 MinInt1 −5.84654 StdMeanInt2 −444.06932 ZeroNgrnd1ratio −111.50951 Canopy10P −145.92581 Canopy50P − 413.21393 Canopy80P	0.74	0.57	28.02	46.68	5.632

Veg = Vegetation lidar hit; Grnd = Ground lidar hit; Int = Intensity associated with lidar hit; Veg1, 2 = 1st, 2nd returns; P_ . . . _10–90 = Percentiles; CV = Coefficient of variation; StdMean = Standard error of the mean; Std = Standard deviation; Canopy 10–90 = Canopy cover percentiles; N..ratio = Vegetation or ground hits as a ratio of return totals; Vegratio = Vegetation hits as a ratio of total hits

the volume and biomass, as well as precision, for the second plot-level segmentation result (0.091 ha/average object) and the result with the highest accuracy for the lidar point height distributional approach (1.885 ha/average object). The 0.091 ha average object size resulted in the best volume and biomass R^2 values in van Aardt *et al.* (2006). These segmentation results were selected based on their compatibility with existing forest sampling methods and to serve as an indication of a best-case volume estimation and object-level classification effort, respectively. Two- and 3-class deciduous, coniferous, and mixed models, as well as a general model, were applied to all objects. Objects unassigned to a class, due to missing model parameter values for those objects, were modeled using the general volume/biomass models and average per-hectare values for that specific segmentation result. Such objects could, for instance, occur when an object exhibited only first and last returns, while the classification model required intermediate return parameters for class assignment. Model estimates were compared to BAF plot estimates for each of the classes and the full area in order to gauge the accuracy and precision of the full-area, per-object classification and estimation approach when compared to an operational method for volume/biomass assignment to forest types.

Results and Discussion

Discriminant Classification using Lidar Point-Height Distributional Variables

Stepwise discriminant analysis was suited to reduction of classification variables from 75 original lidar point-height distributional variables to fewer than 10 variables (Table 4) in each classification attempt. The number of selected variables was considered adequate given that only height and one-wavelength intensity values were available for classification, as opposed to diverse data, e.g., multiple spectral bands. Identified variables were those that best separated classes, while maintaining a low within class variation. Correlation analysis resulted in removal of up to four variables in each classification attempt. Most of the removed variables were related in terms of distributional characteristics, e.g., closely spaced percentile values, while correlations among other variables, e.g., skewness of first return vegetation heights and the 40th canopy cover percentile (3-class; 0.035 ha/average object), were less intuitive. This underlined the importance of complete evaluation of all correlations in order to define the feature space using uncorrelated variables that are most important to class separation, based on partial R^2 values. However, the geographical specificity of selected variables needs to be evaluated in future research.

All types of distributional data types were well represented by the final selected variables. However, intensity values (near-infrared: 1,064 nm) were prevalent, with especially the median intensity of first return vegetation heights present in all data sets. This highlighted the value of per-object, lidar-associated intensity data for lidar-based classification. Near-infrared wavelengths have been shown to be highly discriminant among vegetation types, especially between deciduous and coniferous species (Martin *et al.*, 1998; van Aardt and Wynne, 2001; van Aardt and Wynne, 2007). Other well-represented variables included the standard deviation of second return vegetation heights and the number of first return ground hits as a ratio of total first returns. These variables were indicators of vegetation cover. Second return metrics, which are associated with intermediate returns and by extension lower canopy cover indicators, played a role in defining different forest structures. Large standard deviations for second return vegetation heights can be interpreted to be indicative of a mid-canopy structure with more variable

TABLE 4. FINAL VARIABLES ENTERED INTO LIDAR POINT-HEIGHT-BASED (DISTRIBUTIONAL) DISCRIMINANT CLASSIFICATIONS (2-CLASS = DECIDUOUS-CONIFEROUS). PARTIAL R^2 VALUES ARE GIVEN AFTER EACH VARIABLE AS AN INDICATOR OF RELATIVE IMPORTANCE TO THE CLASSIFICATION

Classification	Final variables entered into discriminant analysis
27,050 objects (0.035 ha/average object)	MaxVeg1(0.40) MedianRef1 (0.09) Grnd2ratio (0.09) MinRef2 (0.03) StdMeanRef2 (0.02)
10,352 objects (0.091 ha/average object)	StdVeg2 (0.32) MedianRef1 (0.17) Grnd2ratio (0.05) MinRef2 (0.02) StdMeanRef2 (0.02) Vegratio (0.02) Canopy50P (0.01)
6,687 objects (0.141 ha/average object)	StdVeg2 (0.33) MedianRef1 (0.17) Veg2ratio (0.05) P_Veg2_30 (0.03) MinVeg2 (0.02) RangeRef2 (0.02) SkewnessVeg1 (0.01)
2,972 objects (0.318 ha/average object)	StdVeg2 (0.33) MedianRef1 (0.15) Grnd1ratio (0.04) MaxRef1 (0.04) CVVeg1 (0.02)
1,473 objects (0.642 ha/average object)	StdVeg2 (0.33) MedianRef1(0.14) ZeroNVeg2ratio (0.03) P_Veg2_30 (0.03) RangeRef1 (0.02) StdRef1 (0.02) Canopy80P (0.01)
981 objects (0.964 ha/average object)	StdVeg2 (0.35) MedianRef1 (0.13) ZeroNgrnd1ratio (0.04) RangeRef1 (0.05) StdMeanVeg2 (0.03) CVVeg2 (0.02) P_Veg2_90 (0.02) KurtosisVeg2 (0.01)
749 objects (1.263 ha/average object)	StdVeg2 (0.34) MedianRef1 (0.13) ZeroNgrnd1ratio (0.05) RangeRef1 (0.05) RangeVeg2 (0.02) Canopy20P (0.02) MinVeg1 (0.01) MaxRef2 (0.01)
502 objects (1.885 ha/average object)	StdVeg2 (0.3693) MeanRef1 (0.1658) ZeroNgrnd1ratio (0.0242) StdRef2 (0.0325) RangeVeg2 (0.0141) StdMeanRef2 (0.0190) CVVeg1 (0.0232) MinVeg2 (0.0113) RangeRef1 (0.0112)
374 objects (2.530 ha/average object)	StdVeg2 (0.35) MeanRef1 (0.11) Canopy60P (0.06) SkewnessVeg1 (0.01) MinVeg2 (0.01) ModeVeg2 (0.01)
240 objects (3.942 ha/average object)	StdVeg2 (0.33) MeanRef1 (0.13) RangeVeg2 (0.02) ModeVeg1 (0.02) MinVeg1 (0.02) Canopy10P (0.02)
168 objects (5.632 ha/average object)	StdVeg2 (0.34) MedianRef1 (0.15) StdMeanRef1 (0.03) MaxRef1 (0.05) MaxVeg2 (0.04) ModeVeg2 (0.03) RangeRef2 (0.03) Canopy10P (0.01) Canopy30P (0.02)
167 Appomattox forest stands (5.666 ha/average object)	MedianRef1 (0.28) P_Veg2_80 (0.18) P_Veg2_10 (0.05) Canopy60P (0.04) Canopy10P (0.03)

Veg = Vegetation lidar hit; Grnd = Ground lidar hit; Ref = Reflectance associated with lidar hit; Veg1, 2 = 1st, 2nd returns; P_ . . . _10–90 = Percentiles; CV = Coefficient of variation; StdMean = Standard error of the mean; Std = Standard deviation; Canopy 10–90 = Canopy cover percentiles; N..ratio = Vegetation or ground hits as a ratio of return totals; Vegratio = Vegetation hits as a ratio of total hits

height values, while the opposite is true of smaller standard deviations. Variables selected by the stepwise discriminant procedure for the best classification result (1.885 ha/average object, 2-class lidar distribution; 89.2 percent accuracy) are shown in Table 4.

Classification accuracies for the point-height-based discriminant classification approach are shown in Figure 4. Overall accuracies ranged from 81.4 percent to 89.2 percent for the 2-class, deciduous-coniferous classification. Producer's and user's accuracies for the deciduous and coniferous classes indicated that deciduous class assignment

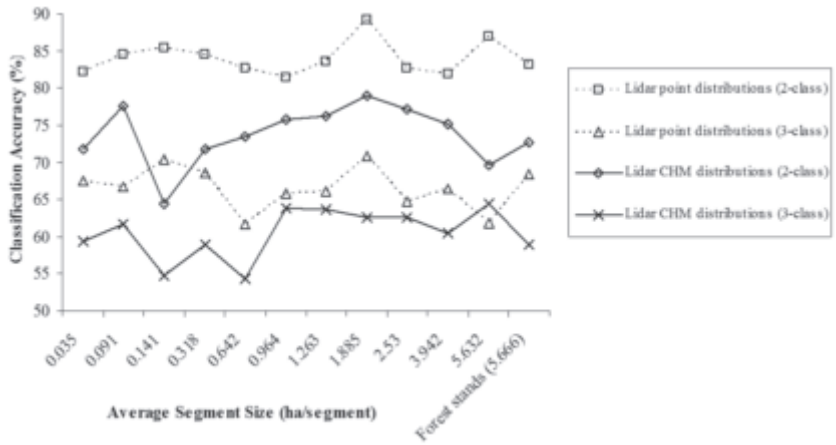

Figure 4. Overall classification accuracies for 2- and 3-class classifications based on lidar points and CHM distributions.

was more reliable than for coniferous objects, both from a map producer's and a map user's perspective. Kappa statistics (Figure 5) for the 2-class classification ranged from 60.2 percent to 76.7 percent. Although overall and Kappa statistics peaked at 1.885 ha/average object, significant differences were only found between 1.885 ha/average object (89.2 percent) and 0.035 ha/average object (82.2 percent) and 0.964 ha/average object (81.4 percent) ($\alpha = 0.05$). Overall accuracies for the 3-class, deciduous-coniferous-mixed classification (Figure 4) ranged from 61.6 percent to 70.8 percent, while the Kappa statistics (Figure 5) varied between 40.4 percent and 53.5 percent. Peak values again were found at the 1.885 ha/average object size. No significant differences were found in the case of the 3-class classification scheme (Table 5). Significance testing indicated that there were minor to non-existing differences within the 2-class and 3-class schemes, but the t-test revealed a significance difference between the mean classification accuracies for the 2- and 3-class schemes at $\alpha = 0.05$ (Table 5). Producer's accuracies generally were highest for coniferous, followed by deciduous and mixed objects. User's accuracies typically decreased from deciduous to coniferous to mixed object classification.

The following findings are particularly noteworthy:

1. The lack of statistical differences among classification results from different object sizes indicated that average object size did not influence classification for the study area. This result was attributed to the hierarchical nature of the segmentation algorithm which merges smaller, homogenous objects to form larger objects at higher hierarchical levels. Within-object variance was therefore already minimized before combination of smaller objects, leading to similar accuracies for all object sizes. A non-hierarchical segmentation approach therefore could be evaluated in future to determine if object size will affect classification accuracies in such a scenario.
2. The significance of the highest accuracies for the 2-class versus 3-class scheme indicated that a deciduous-coniferous forest delineation was better suited to the Virginia Piedmont, as opposed to the inclusion of a mixed category. This was attributed to the forest types found in the study area, with most of the stands represented by one distinct taxonomic group and few completely mixed stands. The mixed class only constituted 25 (11.4 percent) BAF plots when a 75 percent basal area purity cut-off was used, further corroborating this conclusion.
3. There also was no significant difference between object-based classification and classification based on existing forest stands in the study area, in both the 2- and 3-class

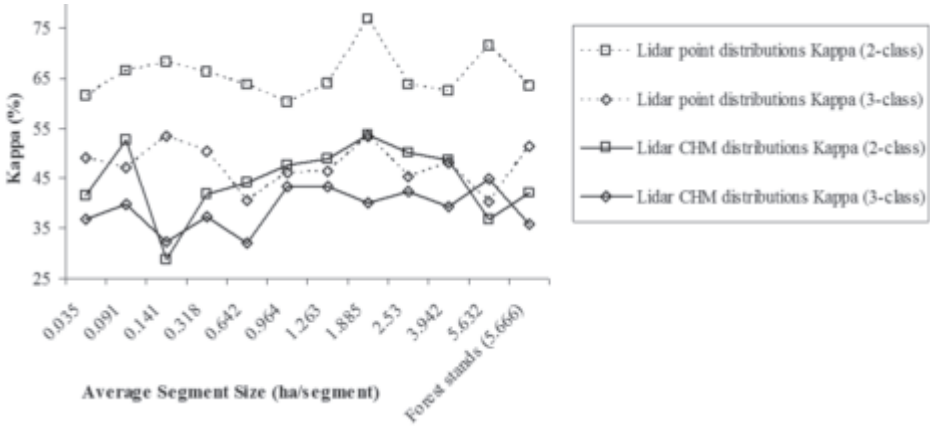

Figure 5. Kappa statistics for 2- and 3-class classification based on lidar points and CHM distributions.

TABLE 5. SIGNIFICANCE RESULTS FOR DISTRIBUTIONAL POINT-HEIGHT-BASED AND CHM-BASED DISCRIMINANT CLASSIFICATIONS ACROSS ALL AVERAGE OBJECT SIZES. ONLY CLASSIFICATIONS FOR AVERAGE OBJECT SIZES THAT ARE SIGNIFICANTLY DIFFERENT FROM THE BEST RESULT ARE INDICATED BY * ($\alpha = 0.05$)

Significance Test		Point-Height-Based Discriminant Classification	CHM-Based Discriminant Classification
z-test: Between average object sizes (Best 2-class lidar points: 1.885 ha/average object; 89.2%)	2-class	2.20* (0.964 ha/average object: 81.4%)	3.27* (0.141 ha/average object: 64.4%)
(Best 2-class CHM-based: 1.885 ha/average object; 79%)		2.03* (0.035 ha/average object: 82.2%)	
	3-class	None	None
Between 2-class and 3-class means (critical two-tail t-test: 2.20)		19.64*	12.96*
Between 2-class means (critical two-tail t-test: 2.20)		7.47*	
Between 3-class means (critical two-tail t-test: 2.20)		4.47*	

schemes. Although unexpected, this result was ascribed to the definition of forest stands in an operational context. Forest stands are more often defined by their species make-up (coniferous-deciduous-mixed) than by their height structure (even-aged versus all-aged). This effectively made the Appomattox stand map a thematic species map. However, the classification of objects was based on forest structure and not forest type definition. van Aardt *et al.* (2006) also found improved adjusted R^2 values for object-based volume and biomass modeling when compared to the operational stands. Object-based classification accuracies therefore were deemed encouraging, especially in the context of associated volume and biomass modeling results.

Discriminant Classification using CHM Height Distributional Variables

Stepwise discriminant analysis again was effective in reducing classification variables from 31 original CHM distributional variables to fewer than 10 variables for both 2- and 3-class classification schemes. As was the case for the point-height-based approach, most distributional data types were well represented, e.g., maximum height, canopy cover percentiles, and the standard deviation of height. Maximum height, the 90th height percentile, and the 20th and 30th canopy cover percentiles were particularly well represented. These variables indicated that structural information, represented by the percentile variables, also was important to forest type definition.

Overall classification accuracies for the CHM-based discriminant classification approach (Figure 4) ranged between 64 percent and 79 percent (2-class), and 54 percent and 64 percent (3-class). Only the results of 1.885 ha/average object (79 percent) and 0.141 ha/average object (64 percent) were significantly different from each other, while there were no significant differences in the 3-class classification scheme ($\alpha = 0.05$). The 2- and 3-class mean accuracies were significantly different from each other at $\alpha = 0.05$ (t-test). This corroborated the results from the point-height-based approach that a 2-class (deciduous-coniferous) scheme is better suited to the study area than a 3-class (deciduous-coniferous-mixed) scheme.

There again was no significant difference between object-based classification and classification based on existing forest stands in the study area, further corroborating results from the point-height-based approach. Kappa statistics (2-class: 29 percent to 54 percent; 3-class: 32 percent to 45 percent), shown in Figure 5, were distinctly lower than those found for the point-height-based approach, indicating that classification using lidar point-height distributions resulted in a generally better forest type assignment than the CHM-based classification. The lidar point height approach was a significant improvement over the CHM approach for the 2- and 3-class forest definitions. However, the first method is computationally more demanding, requiring advanced computer hardware and lidar sensors. The latter approach can be based solely on the single distribution from a forest canopy height model. Results for significance tests are shown in Table 5. Coniferous producer's accuracies were higher than deciduous accuracies for the 3-class forest definition. This was due to a "purer" definition of the coniferous class in the 3-class approach. A 90 percent basal area coniferous majority, as opposed to 51 percent for the 2-class approach, resulted in a definitively purer class. This came at the cost of reduced overall accuracy due to the addition of a mixed class. Class definitions ultimately are the choice of the user, who might be inclined to define Virginia Piedmont forests as a 2-class forest biome, thereby increasing classification accuracies, but sacrificing a more detailed class definition.

A caveat of any distributional approach, namely unclassified objects due to missing classification variables, generally can be circumvented by limiting independent variables to those types that are well represented for all object sizes. Fifth lidar height return values, for instance, were not used as part of the independent variable set. However, only as few as five out of the total 6,687 (0.141 ha/average object) objects will remain unclassified due to missing second return variables. This was attributed to objects, devoid of vegetation, where only first lidar returns were recorded. Unclassified objects were not used as part of the cross-validation accuracy assessment, but operationally should still be addressed through reclassification. Possible solutions to situations where objects have missing classification variables include post-classification photo-interpretation or field verification.

Volume and Biomass Estimation

Results for the volume and biomass estimation, based on objects classified using the models developed in this study, and volume and biomass models developed by van Aardt *et al.* (2006), are shown in Figure 6 (0.091 ha/average object; best volume biomass model results in van Aardt *et al.*, 2006). Although differences between BAF plot and modeling estimates ranged between 26.3 percent and 52.9 percent for separate forest type volume estimations, overall volume estimate differences were between 0.6 percent and 1.5 percent (2-class model), 3.8 percent and 5.5 percent (3-class model), and 0.9 percent and 1.7 percent (general model). Results such as these bode well for potential operational implementation of a combined classification-estimation effort using an object-oriented lidar distributional approach, with especially precision estimates being distinctly lower (16.5 percent to 51.9 percent) for model-based estimation compared to BAF plot results. Further research is still required to evaluate the applicability of associated precision figures to operational scenarios. The largest discrepancies between field-based and modeling estimates occurred in the smaller object (0.035 ha/average object) 2-class coniferous (26.3 percent) and 3-class mixed (52.9 percent) classes. This was attributed to the inherently variable nature of the mixed class, while the 2-class coniferous group exhibited similar behavior in the

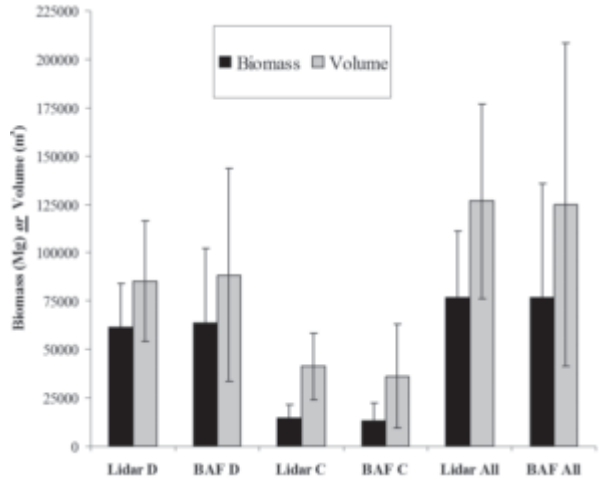

Figure 6. Results of volume and biomass estimations, based on classified objects and volume/biomass models from van Aardt *et al.* (2006) for the full study area and the 0.091 ha/average object segmentation result. Estimate precisions are shown using standard error bars (D = deciduous; C = coniferous).

volume/biomass model development study by van Aardt *et al.* (2006). Similar trends were evident for biomass modeling, with the differences between general BAF plot and model estimation ranging from 0.5 percent to 3.8 percent, and the 2-class coniferous and 3-class mixed classes again exhibiting the largest errors when compared to field estimates.

A distinct difference among modeling results for different object sizes was absent, with the larger object (1.885 ha/average object) estimates being very similar to results obtained for the two-plot level object sizes (0.035 and 0.091 ha/average object). This indicated that an object-oriented, lidar distributional approach to forest type classification and volume and biomass estimation was amenable to object sizes that are large enough to be scaled to operational forest stand sizes. The associated high precisions of the estimates were promising for operational implementation of such an approach, once the relatively high costs associated with lidar data acquisition are addressed. Plate 1 shows a wall-to-wall per-object (0.091 ha/average object) volume estimation for each taxonomic group in the study area.

Conclusions

Per-object classification results, from both lidar point-height-based and CHM-based distributional discriminant classifications, were promising when one considers the type of input data, the variability in natural ecosystems based on basal area contributions for each class, and the classification approach used. Accuracies as high as 89 percent for the point-height-based discriminant classification and 79 percent for the CHM-based approach bode well for lidar-based per-object classification. Higher accuracies for the point-height-based approach were attributed to the increased variable type range, which included more structural (2nd returns) and intensity variables than the CHM-based approach.

There were limited significant differences within classification approaches, indicating that average object size did not influence the outcome. This furthermore implies that reducing the per-object coverage of lidar points would have little to no effect on classification accuracy, with potential implications for a more sampling-oriented approach to lidar-based forest inventories. The absence of a decreasing classification accuracy trend at larger object sizes was attributed to the hierarchical nature of the segmentation algorithm. The algorithm was based on the minimization of within-object variance, but since smaller objects constituted the building blocks for larger objects, variance minimization already was addressed at lower levels. Stand-based classification also was not significantly different from object-based approaches. This was due to the definition of operational forest stands on a per-species or type basis, resulting in an extant forest type map.

Stepwise discriminant analysis, as part of discriminant classification (van Aardt and Wynne, 2001), was confirmed as an effective method for variable reduction. Selected variables included a broad range of distributional data types, while the inclusion of intensity variables highlighted their importance to lidar-based classification approaches. The standard deviation of second return vegetation hits and the first return ground hits as a ratio of total first returns were also well represented variables. Both these metrics were important indicators of vegetative cover.

Two-class forest type definition (deciduous-coniferous) resulted in better accuracies than a 3-class (deciduous-coniferous-mixed) approach for the study area, although

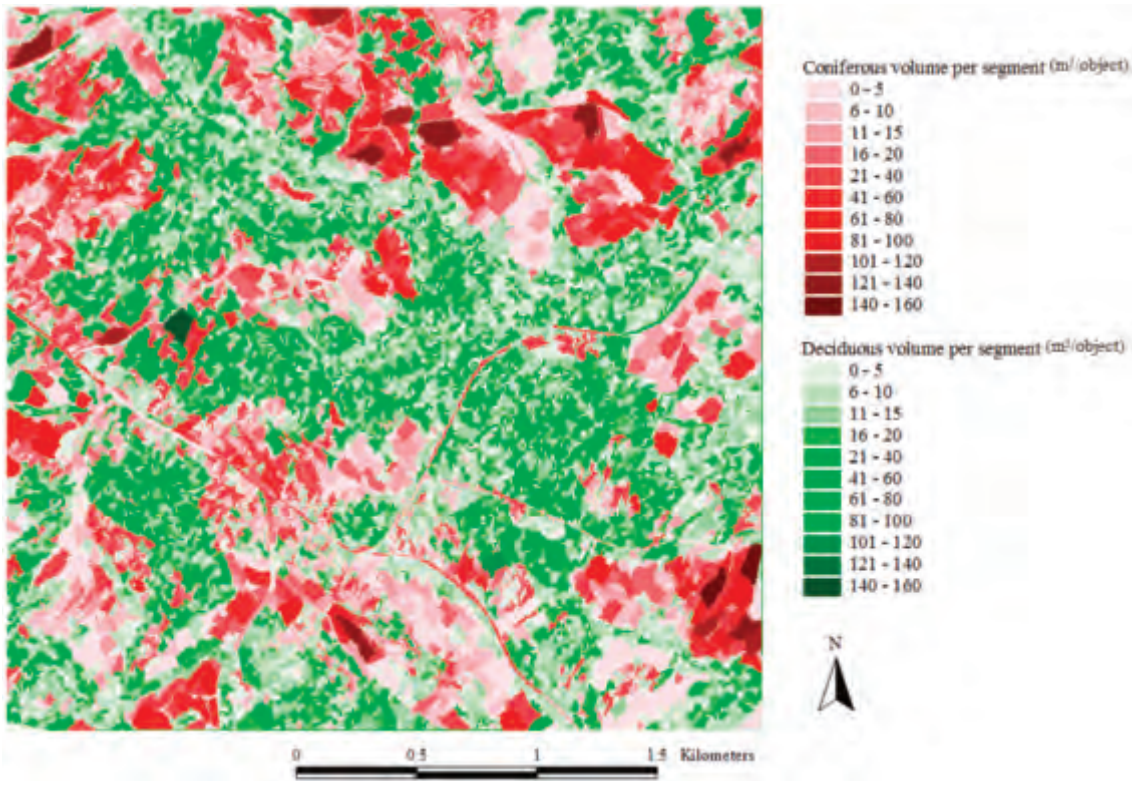

Plate 1. An example of 2-class wall-to-wall per-object volume estimation for the study area using only lidar and field data; object size = 0.091 ha/average object.

an n-class classification approach, where $n > 2$, also has advantages depending on forest management requirements. This result was attributed to high basal area percentages, in terms of deciduous-coniferous mixtures, that had to be used for mixed class definition. The mixed class eventually was closely associated with the deciduous group, thereby reducing deciduous producer's accuracies in the 3-class scheme. Higher producer's accuracies for the coniferous class in the 3-class approach indicated that the deciduous and mixed classes were the main contributors to lower overall accuracies because of increased between-group confusion.

Forest volume and biomass estimation, based on objects classified using the developed approach, showed significant potential for operational implementation. Differences between BAF field plot estimates and forest type model estimates were negligible in most instances, with the 2-class coniferous and 3-class mixed classes warranting further investigation. General volume and biomass model estimates closely approximated field estimates, while the precisions of the estimates were distinctly better using the lidar data than using the BAF plots alone.

Although traditional approaches achieve adequate classification accuracies using multispectral data (Franklin, 1994; White *et al.*, 1995), a lidar-based object-oriented approach has multiple benefits. Lidar data have been used extensively for estimating forest biophysical parameters (Means *et al.*, 2000; Naesset, 2002; Popescu *et al.*, 2002; Bortolot and Wynne, 2005), and coupled with classification, could enable a forest inventory approach that is based on a single data source. Due to their hierarchical nature, object-oriented approaches also have the benefit of recombination of object-level results to fit almost any required scale. Lastly, the simplicity of the approach is attractive, since only per-object height values are potentially required, while co-registration errors between optical and lidar data also are minimized. Extension of accurate classifications to lidar-derived forest volume or biomass-by-type is appealing, and could prove useful in forest inventories. The biggest hurdles to large-scale application are data cost and processing time, which likely will decrease as more data providers emerge and technology improves. Independent of these caveats, analytical approaches are continuously evolving to a stage where multi-source remote sensing data might no longer be required for complete forest inventories.

Acknowledgments

This research was made possible by funding from NASA (Grant # NG65-10548; NG613-03019), the McIntire-Stennis Research Program (Grant # VA-136589), the Forestry Department and Graduate Student Association at Virginia Polytechnic Institute and State University, and the Potomac chapter of the American Society for Photogrammetry and Remote Sensing. Field data collection was supported by the Virginia Department of Forestry, specifically Todd Edgerton, Ralph Toddy, and Wayne Bowman (VDOF). Dr. Sorin Popescu (Texas A&M University) provided invaluable assistance with statistical and lidar analyses. Amy Zhang from the Statistics department at Virginia Polytechnic Institute and State University served as statistical consultant.

References

Abkar A., M.A. Sharifi, and N.J. Mulder, 2000. Likelihood-based image segmentation and classification: A framework for the integration of expert knowledge in image classification procedures, *Journal of Algebraic Geometry*, 2(2):104–119.

Ardö, J., 1992. Volume quantification of coniferous forest compartments using spectral radiance recoded by Landsat Thematic Mapper, *International Journal of Remote Sensing*, 13(9):1779–1786.

Avery, T.E., and H.E. Burkhart, 1994. *Forest Measurements*, Fourth edition. McGraw-Hill, Boston, 408 p.

Baatz, M., and A. Schäpe. 2000. Multiresolution segmentation - An optimization approach for high quality multi-scale image segmentation, *Angewandte Geographische Informationsverarbeitung XII, Beiträge zum AGIT-Symposium Salzburg* (J. Strobl, T. Blaschke, and G. Griesebner, editors), September, Karlsruhe, Herbert Wichmann Verlag, pp. 12–23.

Benz, U.C., P. Hofmann, G. Willhauck, I. Lingenfelder, and M. Heynen, 2004. Multi-resolution, object-oriented fuzzy analysis of remote sensing data for GIS-ready information, *ISPRS Journal of Photogrammetry and Remote Sensing*, 58:239–258.

Bortolot, Z.J, and R.H. Wynne, 2005. Estimating forest biomass using small footprint LiDAR data: An individual tree-based approach that incorporates training data, *ISPRS Journal of Photogrammetry & Remote Sensing*, 59:342–360.

Brandtberg, T. 2007. Classifying individual tree species under leaf-off and leaf-on conditions using airborne lidar, *ISPRS Journal of Photogrammetry and Remote Sensing*, 61:325–340.

Budreski, K.A., R.H. Wynne, J.O. Browder, and J.B. Campbell, 2007. Comparison of segment and pixel-based non-parametric land cover classification in the Brazilian Amazon using multitemporal Landsat TM/ETM+ Imagery, *Photogrammetric Engineering & Remote Sensing*, 73(7):813–827.

Burrough, P.A., and R.A. McDonnell, 1998. *Principles of Geographical Information Systems*, Oxford University Press, Oxford, England, 333 p.

Clark III, A., D.R. Phillips, and D.J. Frederick, 1986. *Weight, Volume, and Physical Properties of Major Hardwood Species in the Piedmont*, USDA Forest Service, Southeastern Forest Experiment Station Research Paper SE-255, June.

Congalton, R.G., and K. Green, 1999), *Assessing the Accuracy of Remotely Sensed Data: Principles and Practices*, Lewis Publishers, New York, 137 p.

Cortijo, F.J., and N.P. De la Blanca, 1999. The performance of regularized discriminant analysis versus non-parametric classifiers applied to high-dimensional image classification, *International Journal of Remote Sensing*, 20(17):3345–3365.

Dorren, L.K.A, Maier, B., and A.C. Seijmonsbergen, 2003. Improved Landsat-based forest mapping in steep mountainous terrain using object-based classification, *Forest Ecology and Management*, 183(2003):31–46.

Douglas, T.E., D.L. Evans, K.L. Belli, and S.D. Roberts, 2003. Classification of pine and hardwood by the distribution and intensity of lidar returns, *Proceedings of the ISPRS Workshop - Three Dimensional Mapping from InSAR and LIDAR*, June 17–19, Portland, Oregon, unpaginated CD-ROM.

eCognition User's Manual, 2003. Definiens Imaging, URL: www.definiens.com (last date accessed: 10 April 2008).

Foody, G.M., 2004. Thematic map comparison: Evaluating the statistical significance of differences in classification accuracy, *Photogrammetric Engineering & Remote Sensing*, 70(5):627–633.

Franklin, S.E., 1994. Discrimination of subalpine forest species and canopy density using digital CASI, SPOT PLA and Landsat TM data, *Photogrammetric Engineering & Remote Sensing*, 60(10):1233–1241.

Heyman, O., G.G. Gaston, A.J. Kimerling, and J.T. Campbell, 2003. A per-segment approach to improving Aspen mapping from high-resolution remote sensing imagery, *Journal of Forestry*, 101(4):29–33.

Jaakkola S.P., 1989. Applicability of SPOT for forest management, *Advanced Space Research*, 9(1):135–141.

Kayitakire, F., C. Farcy, and P. Defourny, 2002. Ikonos-2 imagery potential for forest stands mapping, *Proceedings of the Forest-SAT Symposium*, Heriot Watt University, Edinburgh, 05–09 August, unpaginated CD-ROM.

Kressler, F., Y. Kim, and K. Steinnocher, 2003. Object-oriented land cover classification of panchromatic KOMPSAT-1 and SPOT-5 data, *Proceedings of IGARSS 2003 IEEE*, Toulouse, unpaginated CD-ROM.

Lefsky, M.A., W.B. Cohen, S.A. Acker, G.G. Parker, T.A. Spies, and D. Harding, 1999. Lidar remote sensing of the canopy structure and biophysical properties of Douglas-fir and western hemlock forests, *Remote Sensing of Environment*, 70:339–361.

Li W., G.B. Benie, D.C. He, S. Wang, D. Ziou, and Q.H.J. Gwyn, 1999. Watershed-based hierarchical SAR image segmentation, *International Journal of Remote Sensing*, 20(17):3377–3390.

Martin, M.E., S.D. Newman, J.D. Aber, and R.G. Congalton, 1998. Determining forest species composition using high spectral resolution remote sensing data, *Remote Sensing of Environment*, 65:249–254.

Means J.E., S.A. Acker, B.J. Fitt, M. Renslow, L. Emerson, and C.J. Hendrix, 2000. Predicting forest stand characteristics with airborne scanning lidar, *Photogrammetric Engineering & Remote Sensing*, 66(11):1367–1371.

Naesset, E., 2002. Predicting forest stand characteristics with airborne scanning laser using a practical two-stage procedure and field data, *Remote Sensing of Environment*, 80(2002):88–99.

Nelson, R., W. Krabill, and J. Tonelli, 1988. Estimating forest biomass and volume using airborne laser data, *Remote Sensing of Environment*, 24:247–267.

Nugroho, M., D.H. Hoekman, and R. De Kok, 2002. Analysis of the forests spatial structure using SAR and Ikonos data, *Proceedings of the ForestSAT Symposium*, Heriot Watt University, Edinburgh, 05–09 August, unpaginated CD-ROM.

Ott, L.R., 1993. *An Introduction to Statistical Methods and Data Analysis*, Duxbury Press, Belmont, California, 1051 p.

Pekkarinen, A., 2002. Image segment-based spectral features in the estimation of timber volume, *Remote Sensing of Environment*, 82:349–359.

Popescu, S.C., R.H. Wynne, and R.F. Nelson, 2002. Estimating plot-level tree heights with lidar: Local filtering with a canopy-height based variable window size, *Computers and Electronics in Agriculture*, 37(2002):71–95.

Popescu, S.C., R.H. Wynne, and J.A. Scrivani, 2004. Fusion of small-footprint lidar and multispectral data to estimate plot-level volume and biomass in deciduous and pine forests in Virginia, U.S.A., *Forest Science*, 50(4):551–565.

Saucier, R.J., and A. Clark III, 1985. *Tables for Estimating Total Tree and Product Weight and Volume of Major Southern Tree Species and Species Groups*, Southwide Energy Committee, American Pulpwood Association, Inc., Rockville, Maryland.

Schroeder, P., S. Brown J. Mo, R. Birdsey, and C. Cieszewski, 1997. Biomass estimation for temperate broadleaf forests of the United States using inventory data, *Forest Science*, 43:424–434.

Shandley, J., J. Franklin, and T. White, 1996. Testing the Woodcock-Harward image segmentation algorithm in an area of southern California chaparral and woodland vegetation, *International Journal of Remote Sensing*, 17(5):983–1004.

Shankar B.U., C.A. Murthy, and S.K. Pal, 1998. A new gray level based Hough transform for region extraction: An application to IRS images, *Pattern Recognition Letters*, 19(1998):197–204.

Sharma, M., and R.G. Oderwald, 2001. Dimensionally compatible volume and taper equations, *Canadian Journal of Forest Research*, 31(5):797–803.

Smits, P.C., and S.G. Dellepaine, 1997. An irregular region label model for multi-channel image segmentation, *Patter Recognition Letters*, 18(1997):1133–1142.

van Aardt, J.A.N., and R.H. Wynne, 2001. Spectral separability among six southern tree species, *Photogrammetric Engineering & Remote Sensing*, 67(12):1367–1375.

van Aardt, J.A.N., R.H. Wynne, and R.G. Oderwald, 2006. Forest volume and biomass estimation using small-footprint lidar-distributional parameters on a per-segment basis, *Forest Science*, 52(6):636–649.

van Aardt, J.A.N., and R.H. Wynne, 2007. Examining pine spectral separability using hyperspectral data from an airborne sensor: An extension of field-based results, *International Journal of Remote Sensing*, 28(2):431–436.

White, J.D., C.K. Glenn, and J.E. Pinder III, 1995. Forest mapping at Lassen Volcanic National Park, California, using Landsat TM data and a geographical information system, *Photogrammetric Engineering & Remote Sensing*, 61(3):299–305.

Wu, J., 1999. Hierarchy and scaling: Extrapolating information along a scaling ladder, *Canadian Journal of Remote Sensing*, 25:367–380.